ACSS2-mediated acetyl-CoA synthesis from acetate is necessary for human cytomegalovirus infection

Anna Vysochan[a,b,1], Arjun Sengupta[c,d], Aalim M. Weljie[c,d], James C. Alwine[a,b], and Yongjun Yu[a,b,2]

[a]Department of Cancer Biology, Perelman School of Medicine, University of Pennsylvania, Philadelphia, PA 19104; [b]Abramson Family Cancer Research Institute, Perelman School of Medicine, University of Pennsylvania, Philadelphia, PA 19104; [c]Department of Pharmacology, Perelman School of Medicine, University of Pennsylvania, Philadelphia, PA 19104; and [d]Institute of Translational Medicine and Therapeutics, Perelman School of Medicine, University of Pennsylvania, Philadelphia, PA 19104

Edited by Thomas E. Shenk, Princeton University, Princeton, NJ, and approved January 17, 2017 (received for review August 26, 2016)

Recent studies have shown that human cytomegalovirus (HCMV) can induce a robust increase in lipid synthesis which is critical for the success of infection. In mammalian cells the central precursor for lipid biosynthesis, cytosolic acetyl CoA (Ac-CoA), is produced by ATP-citrate lyase (ACLY) from mitochondria-derived citrate or by acetyl-CoA synthetase short-chain family member 2 (ACSS2) from acetate. It has been reported that ACLY is the primary enzyme involved in making cytosolic Ac-CoA in cells with abundant nutrients. However, using CRISPR/Cas9 technology, we have shown that ACLY is not essential for HCMV growth and virally induced lipogenesis. Instead, we found that in HCMV-infected cells glucose carbon can be used for lipid synthesis by both ACLY and ACSS2 reactions. Further, the ACSS2 reaction can compensate for the loss of ACLY. However, in ACSS2-KO human fibroblasts both HCMV-induced lipogenesis from glucose and viral growth were sharply reduced. This reduction suggests that glucose-derived acetate is being used to synthesize cytosolic Ac-CoA by ACSS2. Previous studies have not established a mechanism for the production of acetate directly from glucose metabolism. Here we show that HCMV-infected cells produce more glucose-derived pyruvate, which can be converted to acetate through a nonenzymatic mechanism.

human cytomegalovirus | ACLY | ACSS2 | acetate | Acetyl-CoA

Human CMV (HCMV), a human beta herpesvirus, is a significant pathogen which infects most of the human population. It is the most common cause for congenital infection in developed countries, frequently leading to deafness, mental retardation, and developmental disability (1). Additionally, it can be life-threatening for immunocompromised individuals such as organ transplant recipients (2, 3). HCMV infection also has been implicated in atherosclerosis (4) and cancer (5). Studies from our laboratory and others have shown that HCMV infection induces a high level of lipogenesis, which is essential for sustaining the infection (6, 7). This increased lipogenesis is facilitated by HCMV-mediated induction of the sterol regulatory element binding proteins (SREBPs) and carbohydrate-response element binding protein (ChREBP), transcriptional factors that increase the expression of key lipogenic genes (6, 8, 9). The ChREBPs are also key regulators of glucose metabolism; their activation in HCMV-infected cells induces the expression of glucose transporters 4 and 2 (GLUT4 and GLUT2) and glycolytic enzymes, resulting in increased glucose flux which facilitates a metabolic switch for glucose from catabolic energy production to anabolic biosynthesis (9).

Acetyl CoA (Ac-CoA) is a key metabolic intermediate for mammalian cells (10). Cytosolic Ac-CoA is the central precursor for fatty acid and cholesterol biosynthesis. In normal cells with sufficient nutrients, glycolysis converts glucose to pyruvate (Fig. 1*A*), which enters the mitochondria and is converted to Ac-CoA by pyruvate dehydrogenase (PDH). Because mitochondrial Ac-CoA cannot enter the cytoplasm, it is combined with oxaloacetic acid (OAA) to form citrate as part of the tricarboxylic acid (TCA) cycle; citrate can be transported to the cytoplasm via the mitochondrial citrate shuttle. In the cytoplasm the citrate can be converted back to Ac-CoA and OAA by ATP-citrate lyase (ACLY), which has been reported to be the primary enzyme involved in making cytosolic Ac-CoA (11–13).

Under low-glucose, nutrient-restricted conditions, such as fasting or starvation, cytosolic Ac-CoA also can be made from acetate by acetyl-CoA synthetase short-chain family member 2 (ACSS2) (Fig. 1*A*) (13). Acetate plays an important role in maintaining energy homeostasis in mammals. Recent studies have shown that free acetate is an essential carbon source for lipogenesis in cancer cells under stress conditions (14–16). In mammals, acetate can be derived from a number of different sources. It can be obtained exogenously from foods or formed by the gut flora and then further absorbed and used in metabolism (17, 18). Acetate also can be produced endogenously from ethanol metabolism (19), deacetylation of acetylated proteins (20) or acetylcholine (21), and fatty acid β-oxidation in hibernating animals (22). There is no known metabolic mechanism for the production of acetate directly from glucose.

In this study, we report that ACLY and ACSS2 are both activated to produce cytosolic Ac-CoA from glucose carbon for lipogenesis during HCMV infection. However, ACLY can be knocked out with no effect on lipogenesis and HCMV growth. However, we show that ACSS2 is necessary during HCMV infection and can compensate for the loss of ACLY. Our data show that a major means of using glucose carbon for lipogenesis is through acetate and the ACSS2 reaction. Thus, HCMV uses means to produce acetate from glucose. One means of doing so is by converting glucose-derived pyruvate to acetate through nonenzymatic reactions.

Significance

Viruses rely completely on host cell metabolism to provide the building blocks and energy required for producing progeny virions. Infection by human cytomegalovirus (HCMV) induces significant alterations in glucose metabolism by increasing glucose uptake and glycolysis as well as redirecting glucose carbon to support the synthesis of biomolecules such as lipids. The significance of acetate as a nutrient has been ignored for a long period. Our studies show that glucose carbon can be converted to acetate and used to make cytosolic acetyl-CoA by acetyl-CoA synthetase short-chain family member 2 (ACSS2) for lipid synthesis, which is important for HCMV-induced lipogenesis and the viral growth. The study provides greater understanding of HCMV pathogenesis and suggests strategies to develop antiviral therapies.

Author contributions: A.M.W., J.C.A., and Y.Y. designed research; A.V., A.S., and Y.Y. performed research; A.V., A.S., A.M.W., J.C.A., and Y.Y. analyzed data; and J.C.A. and Y.Y. wrote the paper.

The authors declare no conflict of interest.

This article is a PNAS Direct Submission.

[1]Present address: National Medical Services, Inc., NMS Labs, Willow Grove, PA 19090.

[2]To whom correspondence should be addressed. Email: yongjun@mail.med.upenn.edu.

This article contains supporting information online at www.pnas.org/lookup/suppl/doi:10.1073/pnas.1614268114/-/DCSupplemental.

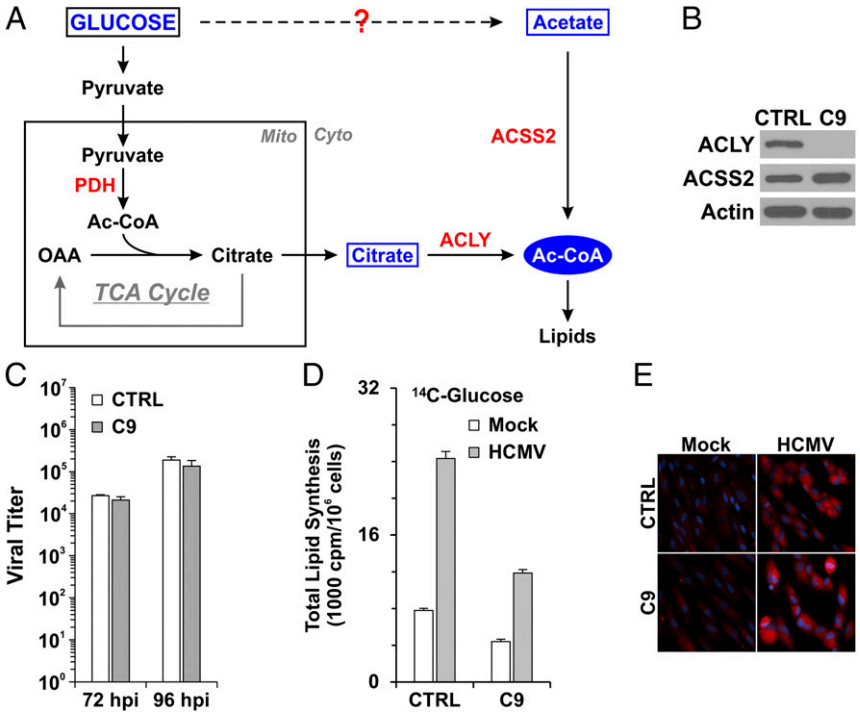

Fig. 1. ACLY is not essential for HCMV-induced lipogenesis. (*A*) Diagram of the synthesis of cytosolic Ac-CoA in mammalian cells; see text for details. (*B*) Protein levels of ACLY and ACSS2 in control HFs (CTRL) expressing a control sgRNA-targeting luciferase gene and the C9 HF line in which ACLY was knocked out. (*C*) ACLY knockout had little effect on HCMV growth in HFs. Confluent control and ACLY-KO C9 HFs were serum-starved and infected by HCMV at an MOI of 3. HCMV viral titers were examined at 72 and 96 hpi. (*D*) ACLY knockout reduced de novo lipid synthesis from glucose carbon by 50%. ACLY-KO cells and control HFs were mock-infected or were infected by HCMV at an MOI of 3. At 48 h, uninfected and infected cells were labeled with [U-^{14}C]-D-glucose for 24 h; total lipids were extracted at 72 hpi and were counted by scintillation counter. Data are shown as the mean ± SD of triplicates. See details in *Materials and Methods*. (*E*) ACLY knockout had little effect on total cellular lipid levels in both mock- and HCMV-infected cells as measured by lipid droplet staining using BODIPY 558/568 C_{12}.

Results

ACLY Is Not Necessary for HCMV Infection and Virally Induced Lipogenesis. We have shown previously that ACLY RNA and protein levels are increased in HCMV-infected cells (6, 23). ACLY can also be activated by cAMP-dependent protein kinase A (PKA) and protein kinase B (Akt) phosphorylation at Ser455 (24, 25). In addition to its increased expression during HCMV infection, our data also show that phosphorylation of ACLY at Ser455 is greatly increased after HCMV infection (23). These data suggest that ACLY is activated and possibly plays an important role in HCMV growth and HCMV-induced lipogenesis. To test this hypothesis, the CRISPR/Cas9 system was used to create an ACLY-KO human fibroblast (HF) cell line called "C9." Sequencing analysis showed that guide RNA created a 4-bp deletion in ACLY exon 3 (Fig. S1*A*) resulting in an ORF shift and the loss of ACLY protein expression in C9 HFs (Fig. 1*B*). Cell proliferation of C9 HFs was slightly slower than that of control HFs (Fig. S2). Confluent control and C9 cells were infected with HCMV to test the effect of ACLY knockout on viral growth. Surprisingly, viral titration results showed that HCMV growth was barely affected in C9 cells as compared with control HFs (Fig. 1*C*). Because ACLY is the primary enzyme producing cytosolic Ac-CoA for lipid synthesis, we tested de novo lipid synthesis from glucose carbon in HCMV-infected C9 cells. In agreement with our previous studies (6, 9, 26), serum-starved control HFs had a low level of lipid synthesis from glucose, which was increased significantly after HCMV infection (Fig. 1*D*). The ACLY knockout in C9 cells reduced de novo lipid synthesis from glucose carbon by 40% and 50% in mock- and HCMV-infected HFs, respectively. This result suggests that in infected cells at least 50% of the glucose carbon used for lipid synthesis is through pathways other than ACLY. To analyze this possibility further, we examined total lipid levels in infected cells by measuring lipid droplet levels using a fluorescent lipophilic dye BODIPY 558/568 C_{12} as previously described (6). In control HFs HCMV infection increased lipid droplet levels significantly (Fig. 1*E*), as we have reported previously (6, 26). Interestingly, in HCMV-infected C9 cells lipid droplet levels were equivalent to the levels in controls (Fig. 1*E*), indicating that ACLY is not essential to maintain high levels of lipogenesis in HCMV-infected cells. This finding is in agreement with there being no effect on viral growth in the C9 cells (Fig. 1*C*) and was confirmed by measuring levels of free fatty acids, which showed that control and C9 HFs infected with HCMV showed equivalent increases in free fatty acids (Fig. S3*A*).

Taken together, these data suggest that HCMV growth and virally induced lipogenesis can be maintained independently of ACLY; thus an alternative means for producing cytosolic Ac-CoA must be in play that can compensate for ACLY loss.

ACSS2-Dependent Utilization of Acetate for Lipogenesis Is Increased in HCMV-Infected Cells and Is Needed for HCMV Growth and Lipid Synthesis from Glucose. It has been shown that under nutrient-restricted conditions cytosolic acetate can be used to synthesize Ac-CoA by ACSS2, which is located in the cytoplasm and nucleus (13, 27). Fig. 2*A* shows that HFs contain ACSS2 and that its levels are maintained during HCMV infection; additionally, ACSS2 protein level was slightly increased in ACLY-KO C9 HFs compared with control HFs (Fig. 1*B*). Fig. 2*B* shows that the utilization of acetate carbon for lipogenesis is increased at least threefold in HCMV-infected HFs, suggesting that ACSS2 is activated in HCMV infected HFs.

To determine the role of ACSS2 in lipogenesis in HCMV-infected cells, we created two ACSS2-KO HF lines, C3 and C11 (Fig. 3*A*), using single-guide RNAs (sgRNAs) to ACSS2 with CRISPR/Cas9 technology. In C3 and C11 HFs, no ACSS2 protein expression was detected (Fig. 3*A*). PCR amplification and

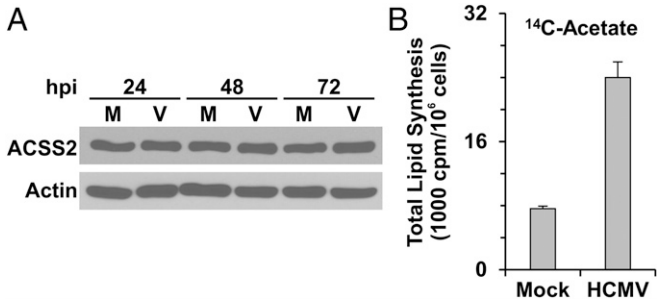

Fig. 2. Acetate utilization for lipogenesis is increased in HCMV-infected cells. (*A*) ACSS2 protein levels in mock- and HCMV-infected cells were unchanged over an infection time course. Whole-cell extracts from mock- and HCMV-infected cells at 24, 48, and 72 hpi were analyzed by Western blot to determine the levels of ACSS2. M, mock infection; V, HCMV infection. (*B*) Lipid synthesis from acetate carbon is increased in HCMV-infected HFs. At 48 hpi, mock- and HCMV-infected HFs were labeled with 1.0 μCi/mL [1, 2-^{14}C2]-acetate (~8.8 μM [1, 2-^{14}C2]-acetate) in serum-free DMEM for 2 h. Then total lipids were extracted and counted in a scintillation counter. Data are shown as the mean ± SD of triplicates.

sequencing results showed that there was a significant deletion in exon 1 of the ACSS2 gene in C3 HFs (Fig. S1 *B* and *C*), and a single nucleotide guanine was inserted in the guide RNA targeting region in exon 2 of the ACSS2 gene in C11 HFs (Fig. S1*D*). In both C3 and C11 HFs, protein levels of ACLY were not affected by ACSS2 knockout (Fig. 3*A*). These ACSS2-KO cells grew significantly more slowly than the control HFs and ACLY-KO C9 cells (Fig. S2), suggesting that ACSS2 is important for growth of HFs under normal tissue-culture conditions. It should be noted that it was not possible to make viable cell lines with both ACSS2 and ACLY knocked out. Thus, in the studies below in which we tested the effects of both ACLY and ACSS2, we depleted ACLY temporarily using an effective shRNA (shACLY) (Fig. 3*B*) in the ACSS2-KO cell lines. Control, C3, and C11 cells were grown to confluency and infected with HCMV to test the effect of ACSS2 knockout, plus or minus ACLY depletion, on viral growth. Fig. 3*C* (white bars) shows that ACSS2 knockout in C3 and C11 cells caused a 10- to 20-fold decrease in viral titer at 96 h post infection (hpi). ACLY depletion in control HFs expressing a single guide RNA specific for luciferase gene (sgLUC) had little effect on titer, in agreement with the results described above in ACLY-KO cells (Fig. 1*C*, gray bars). However, ACLY depletion in ACSS2-KO C3 and C11 cells resulted in an overall 100-fold decrease in viral titers (Fig. 3*C*, gray bars), suggesting that ACLY activity becomes significant in the absence of ACSS2. The corollary of this idea is that ACSS2 activity can compensate for ACLY loss in HCMV-infected cells as measured by viral titers (Figs. 1*C* and 3*C*).

For further confirmation that the reduction of viral titers in C3 and C11 HFs is caused by ACSS2 knockout, silent mutations were introduced into His-tagged human ACSS2 cDNA to mutate both guide RNA targeting sites (Fig. S4*A*). A lentiviral vector expressing His-ACSS2 was constructed using this His-tagged sgACSS2-resistant ACSS2 cDNA (His-ACSS2-R) to infect control, C3, and C11 HFs (Fig. S4*B*). In HCMV-infected control HFs, expression of His-ACSS2 had little effect on viral titer; in HCMV-infected C3 and C11 HFs, the reduction of viral titers was largely rescued by the expression of His-ACSS2 (Fig. S4*C*), indicating that the reduction of viral growth in ACSS2-KO HFs is caused specifically by the loss of ACSS2 expression.

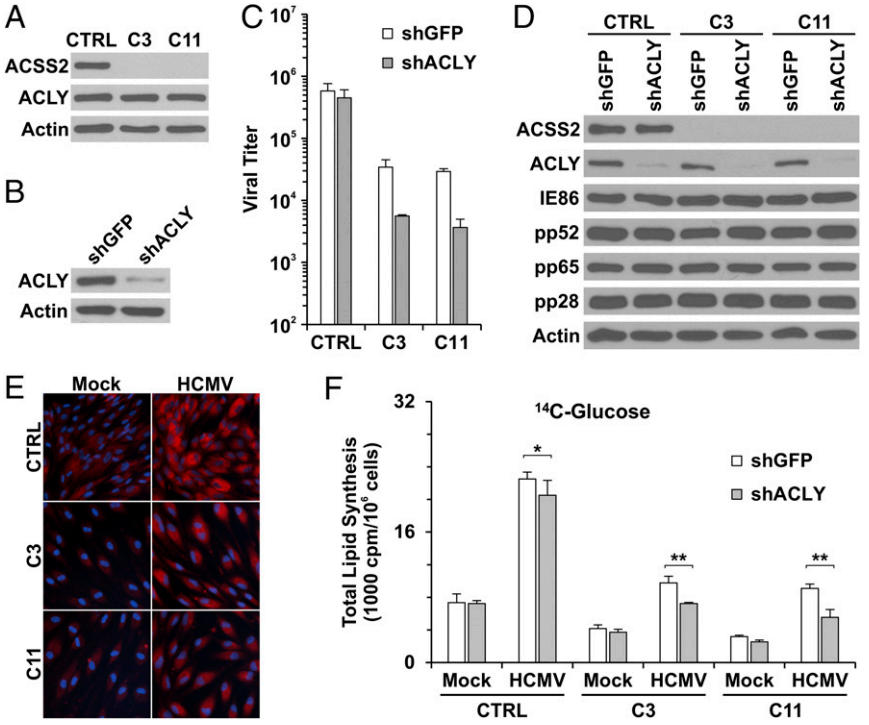

Fig. 3. Knockout of ACSS2 reduces HCMV growth and virally induced lipogenesis in HFs. (*A*) Protein levels of ACSS2 in control and the ACSS2-KO HF cell lines C3 and C11. (*B*) Depletion of ACLY by shRNA in HFs. (*C*) HCMV viral titers at 96 hpi in control and the ACSS2-KO C3 and C11 cell lines treated with either shGFP or shACLY. (*D*) HCMV viral protein expression in control and ACSS2-KO C3 and C11 cell lines at 72 hpi. (*E*) The ACSS2-KO cell lines C3 and C11 show reduced lipid droplet levels in both mock and HCMV infection compared with control HFs. (*F*) Knockout of ACSS2 has a major effect on reducing lipid synthesis from glucose carbon in mock- and HCMV-infected HFs, and further depletion of ACLY shows an additional minor effect. Control and the ACSS2-KO cell lines C3 and C11 were depleted of ACLY using shACLY or were treated with shGFP followed by mock or HCMV infection at an MOI of 3. Lipid synthesis was assayed as described in *Materials and Methods*. Data are expressed as the mean ± SD of triplicates. The Student's *t* test is paired with two-tailed distribution. *$P > 0.1$; **$P < 0.05$.

Examination of viral protein expression showed that an immediate-early protein (IE86), an early protein (pp52), and two late proteins (pp65 and pp28) all had similar levels in control cells, ACSS2-KO cells, and ACSS2-KO/ACLY-depleted cells (Fig. 3*D*). These data show that ACSS2 knockout and/or ACLY depletion does not affect viral gene expression, suggesting that the effect of ACSS2 knockout and ACLY depletion is on virion maturation, where increased lipogenesis is required for membrane formation, as we have shown in previous studies (6, 26).

In ACSS2-KO cells, acetate is no longer used for producing cytosolic Ac-CoA and thereafter lipid synthesis; therefore ACSS2 knockout may result in the accumulation of high levels of acetate that could be cytotoxic. Because acetate can be transported in and out of cells by highly efficient transporters, such as monocarboxylate transporter (MCT) 1 (28), we collected the cultured medium to measure acetate levels by NMR spectroscopy. Fig. S5*A* shows a representative NMR spectrum of acetate. Our tests showed that 200 μM of acetate was detected in the cultured growth medium of control HFs and that the levels of acetate were increased only slightly, to 250 μM, in the cultured growth medium of C3 and C11 HFs (Fig. S5*B*). We found that neither the proliferation of HFs nor viral growth was affected in culture medium supplemented with this level of acetate (Fig. S5 *C* and *D*), suggesting that the inhibition of cell growth and viral replication by ACSS2 knockout is not caused by the increase in acetate.

We next examined total cellular lipid levels by measuring lipid droplets using the lipophilic dye BODIPY 558/568 C_{12} as described in Fig. 1*E*. In agreement with Fig. 1*E*, HCMV infection increased lipid droplet levels in control HFs compared with mock-infected control HFs (Fig. 3*E*). However, lipid droplet levels were lowered in both mock- and HCMV-infected C3 and C11 ACSS2-KO cell lines (Fig. 3*E*). This lowering also was confirmed by levels of free fatty acids in control and ACSS2-KO HFs (Fig. S3*B*). We found that levels of free fatty acids were reduced only~20% in mock-infected C3 and C11 HFs but were reduced by more than 40% in HCMV-infected C3 and C11 HFs compared with HCMV-infected control HFs (Fig. S3*B*). These data suggest that total lipogenesis is decreased by the ACSS2 knockout in infected HFs.

We next examined the effect of ACSS2 knockout on the utilization of glucose carbon for lipogenesis in mock-infected and infected control, C3, and C11 cells. Fig. 3*F* (white bars) reiterated the HCMV-mediated induction of glucose carbon utilization for lipogenesis (compare mock- and HCMV-infected control cells in Fig. 3*F*). However, in the C3 and C11 ACSS2-KO cells, the HCMV-mediated induction was decreased at least 60%. This result suggests that the ACSS2 reaction is a major means of using glucose for lipogenesis in infected cells. Interestingly, the utilization of glucose carbon for lipogenesis was reduced nearly 50% in mock-infected C3 and C11 cells compared with mock-infected control HFs, suggesting that glucose-derived acetate is used for Ac-CoA production and lipogenesis in uninfected normal HFs.

In considering the effect of ACLY depletion (Fig. 3*F*, gray bars), we observed that ACLY depletion reduced the HCMV-mediated induction of lipid synthesis from glucose by only 10% in the HCMV-infected control cells. This reduction is less than that observed with the ACLY-KO cells (Fig. 1*D*) and may be the result of incomplete shRNA depletion (Fig. 3*B*). However, ACLY depletion in HCMV-infected C3 and C11 cells had a noticeable effect, reducing lipid synthesis from glucose by 25–40%. This finding again suggests that glucose carbon can be used to produce cytosolic Ac-CoA by both ACLY and ACSS2 in infected HFs, but the effects of ACLY are more apparent when the dominant ACSS2 pathway is inoperative.

Acetate Can Be Produced from Pyruvate in Serum-Free Medium via Rapid Nonenzymatic Reactions Involving Medium Components. The sharp decline in lipid synthesis from glucose carbon in infected ACSS2-KO cells suggests that acetate is produced from glucose metabolism in infected cells. Fig. 4*A* shows acetate production for 24-h periods through an infection time course. Confluent HFs were serum starved for 24 h, followed by HCMV infection in serum-free medium at a multiplicity of infection (MOI) of 3. At 2 hpi, both mock- and HCMV-infected cells were washed once with serum-free medium. Cells were refed with fresh serum-free medium at 0, 24, and 48 hpi, and the culture medium was collected at 24, 48, and 72 hpi to measure acetate production during every 24-h period. In the period from 0–24 hpi, HCMV-infected cells released slightly more acetate into the medium than did mock-infected cells. During the 24–48 and 48–72 hpi periods, less acetate was released from HCMV-infected cells than from mock-infected cells, suggesting a faster rate of intracellular consumption of acetate for lipogenesis or other acetate-fixing reactions in HCMV-infected cells (Fig. 4*A*). Fig. 4*B* shows the effect of replacing glucose with pyruvate in the culture medium. With pyruvate, acetate production was increased in the 24–48 hpi period, suggesting that acetate is readily produced from pyruvate.

To investigate further how acetate is produced from pyruvate metabolism, a metabolic labeling assay was designed to examine if ^{13}C at the third carbon of pyruvate could be transferred to acetate in cells labeled with a stable isotope tracer [3-^{13}C]-pyruvate (Fig. 5*A*). At 48 hpi, normal and infected HFs were labeled with serum-free and glucose-free culture medium supplemented with 1 mM [3-^{13}C]-pyruvate; then the cultured medium was collected at various times to measure [2-^{13}C]-acetate levels by NMR. Surprisingly, we found that ^{13}C-acetate was present at significant levels in the control medium at 0 min incubation (Fig. 5*B*), indicating that ^{13}C-acetate was generated from the pyruvate before the medium was used for cell culture. Recent studies have shown that a low amount of acetate can be detected in fresh serum-free culture medium by a colorimetric assay (29). To determine whether acetate was being derived from pyruvate in the culture medium, we measured acetate levels in fresh serum-free medium using NMR. The level of acetate detected in medium without glucose and pyruvate (Fig. 5*C*) was similar to that reported by Kamphorst et al. (30). However, the acetate level was more than doubled after addition of pyruvate (Fig. 5*C*). These data suggest either that the pyruvate preparation was contaminated with acetate or that acetate can be derived from pyruvate in serum-free medium by a nonenzymatic reaction. To resolve this question, we added the same amount of

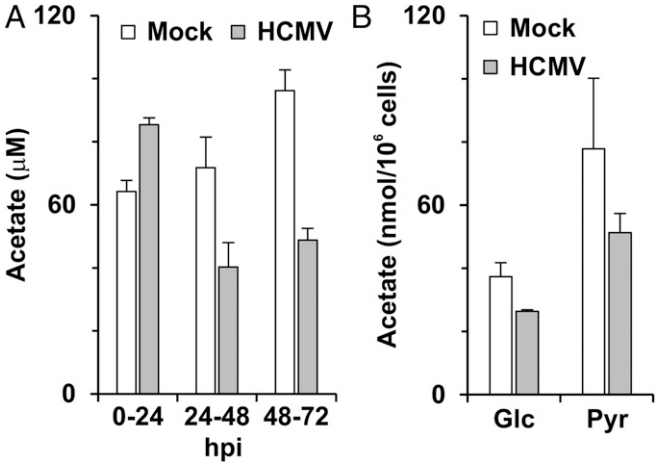

Fig. 4. Acetate production in HFs. (*A*) Acetate levels produced during 24-h periods (0–24, 24–48, and 48–72 hpi) from mock- and HCMV-infected HFs. Data are expressed as the mean + SEM of triplicates. (*B*) Replacing glucose (Glc) with pyruvate (Pyr) in DMEM significantly increases acetate production in both mock- and HCMV-infected HFs. In both cases acetate was quantitated using NMR analysis. Data are expressed as the mean ± SEM of triplicates. See *Materials and Methods* for details.

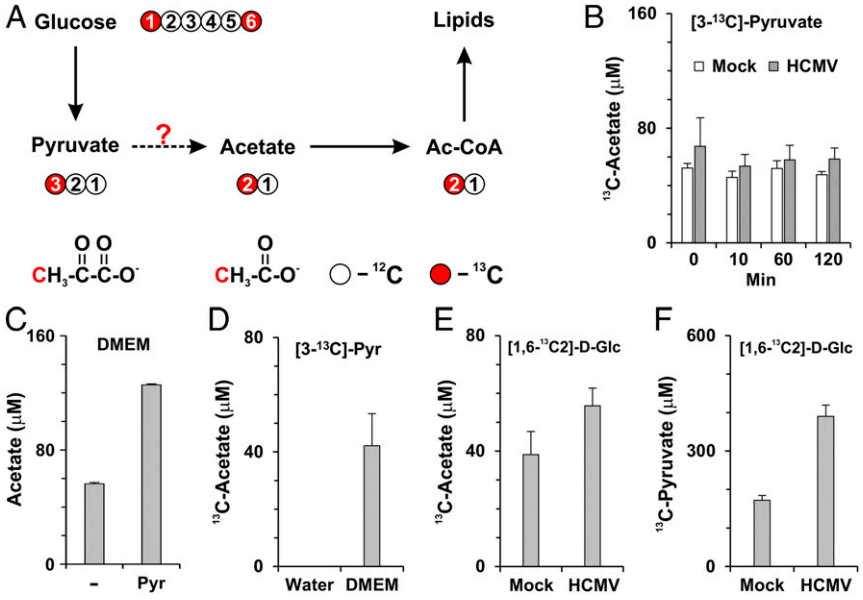

Fig. 5. Conversion of pyruvate to acetate in cell-culture medium. (*A*) Carbon atom transition map depicting labeling patterns of metabolites derived from [1, 6-^{13}C2]-D-glucose. (*B*) Levels of ^{13}C-labeled acetate in the culture medium from cells labeled with [3-^{13}C]-pyruvate. At 48 hpi, mock- and HCMV-infected HFs were labeled with medium containing 1 mM [3-^{13}C]-pyruvate but no glucose. Cultured medium was collected at 0, 10, 60, and 120 min to measure [2-^{13}C]-acetate by NMR. Data are shown as the mean ± SEM of triplicates. (*C*) Acetate levels in fresh serum-free DMEM without glucose in the presence or absence of 1 mM pyruvate. ^{12}C-acetate levels were measured by NMR. Data are shown as the mean ± SEM of triplicates. (*D*) [2-^{13}C]-acetate is produced from [3-^{13}C]-pyruvate added into fresh serum-free medium without glucose. [3-^{13}C]-Pyruvate was freshly added to water or serum-free DMEM without glucose, and the levels of [2-^{13}C]-acetate in water or serum-free medium were measured directly by NMR without cell culture. [2-^{13}C]-acetate is produced from [3-^{13}C]-pyruvate only in medium but not in water. Data are shown as the mean ± SEM of triplicates. (*E*) Levels of [2-^{13}C]-acetate produced from mock- or HCMV-infected cells labeled with [1, 6-^{13}C2]-D-glucose. At 24 hpi, mock- and HCMV-infected cells were replaced with serum-free DMEM containing 5.6 mM [1, 6-^{13}C2]-D-glucose; medium was collected at 48 hpi and analyzed for [2-^{13}C]-acetate levels. Data are shown as the mean ± SD of triplicates. (*F*) Levels of [3-^{13}C]-pyruvate in the same media collected in *E*. Data are shown as the mean ± SD of triplicates.

[3-^{13}C]-pyruvate to water and to fresh, serum-free DMEM for 5 min at room temperature. Then the DMEM and water with [3-^{13}C]-pyruvate were frozen quickly on dry ice without the cell-culture step and were stored at −80 °C before analysis. The ^{13}C-acetate levels then were measured by NMR. We found that ^{13}C-acetate was derived from ^{13}C-pyruvate only in the medium, not in water (Fig. 5*D*), showing that the ^{13}C-acetate was not a contaminant of the ^{13}C-pyruvate stock. These data suggest that medium components catalyze a reaction to convert pyruvate to acetate.

The methyl group of pyruvate can come from C_1 or C_6 of glucose through glycolysis (Fig. 5*A*) (30); thus acetate could be produced from glucose-derived pyruvate. To test this possibility, serum-free DMEM was supplemented with [1,6-^{13}C2]-D-glucose, and cells were cultured in this medium for 24 h beginning at 24 hpi. The medium was collected at 48 hpi to measure ^{13}C-acetate levels. As expected, ∼40 μM of ^{13}C-acetate was produced from mock-infected cells, and ∼40% more ^{13}C-acetate was produced from HCMV-infected cells (Fig. 5*E*). The increased ^{13}C-acetate production in infected cells correlated with the increased ^{13}C-pyruvate caused by the high level of glycolysis in infected cells (Fig. 5*F*). These data suggest that acetate can be produced directly from glucose-derived pyruvate in normal cells and that this production is enhanced in HCMV-infected cells. It should be noted that both pyruvate and acetate are metabolized rapidly in infected cells; thus the steady-state levels shown in Fig. 5 *E* and *F* may not represent the rate of synthesis accurately.

The results reported above suggest that acetate may be derived from pyruvate by nonenzymatic means in serum-free medium. Thus, we sought evidence that acetate could be produced from glucose-derived pyruvate in both normal and infected cultured cells. We postulated that increased levels of glucose-derived pyruvate would result in increased acetate levels in cultured cells. Therefore we debilitated the PDH complex (Fig. 1*A*) in HFs using shRNAs specific for the PDH subunit E1α or a control, shGFP (Fig. 6*A*). PDH E1 is the rate-limiting multimeric subunit in the PDH complex; depletion of its E1α subunit causes loss of activity (31). As expected, PDH inactivation increased the levels of [3-^{13}C]-pyruvate derived from [1,6-^{13}C2]-D-glucose in both mock- and, to a greater extent, HCMV-infected cells (Fig. 6*B*). Fig. 6*C* shows that the increased levels of [3-^{13}C]-pyruvate resulted in increased levels of [2-^{13}C]-acetate. It is likely that the increased utilization of acetate in infected cells results in the lower steady-state level in Fig. 6*C*. These results suggest that glucose carbon can be used to synthesize acetate via pyruvate in HFs and that this synthesis is increased in HCMV-infected cells. Thus, HCMV may use the nonenzymatic mechanism described in Fig. 5 or another, yet to be determined, mechanism. Finally, Fig. 6*D* shows that the depletion of PDH E1α resulted in a 50% reduction in the utilization of glucose carbon for total lipid synthesis in HCMV-infected cells. This is the same effect we noted for the loss of ACLY activity (Fig. 1*D*) and was expected, because ACLY is downstream of PDH. Unlike the loss of ACLY, which has little effect on HCMV growth (Figs. 1*C* and 3*C*), we found that viral titer was reduced 10- to 40-fold in HFs depleted of PDH E1α (Fig. 6*E*). Recent studies have shown that the depletion of PDH E1α not only reduces the intracellular abundance of citrate but also reduces the production of mitochondrial acetyl-CoA for the TCA cycle, resulting in the disruption of central carbon metabolism and energy production in the mitochondria (31). PDH E1α-deficient cells are much more vulnerable to glutamine deprivation and are more reliant on extracellular lipids (31, 32); thus it is reasonable that the depletion of PDH E1α profoundly impacts cellular metabolism and limits viral growth.

Discussion

Ac-CoA is a key metabolic intermediate for bioenergetics and anabolic function. It is a central precursor for lipid synthesis, a precursor of anabolic reactions, an allosteric regulator of enzymatic activities, a key determinant of protein acetylation, including

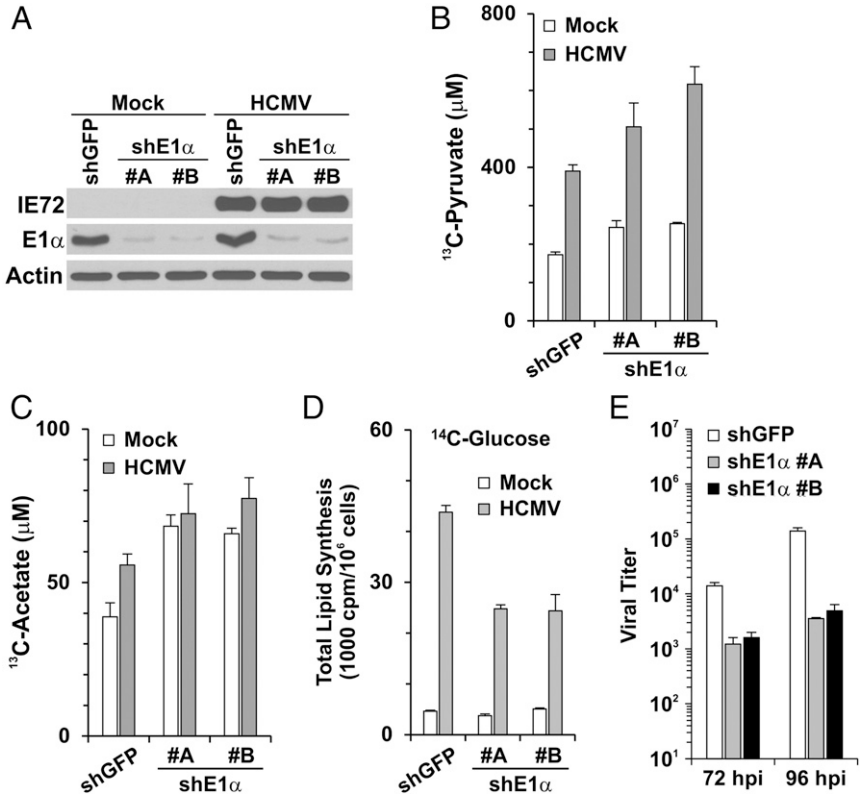

Fig. 6. Acetate production and lipid synthesis from glucose in HFs depleted of PDH. (*A*) Depletion of PDH E1α in mock- and HCMV-infected HFs using two different shRNAs, shE1α #A and #B. (*B* and *C*) Depletion of PDH increased the accumulation of pyruvate and acetate derived from glucose in mock- and HCMV-infected HFs. HFs were treated with shGFP (control) or shE1α for 3 d, followed by serum starvation for 1 d. Cells then were mock or HCMV infected in serum-free DMEM. At 24 hpi the cells were labeled with 5.6 mM [1, 6-^{13}C2]-D-glucose in serum-free DMEM. At 48 hpi the medium was collected for NMR quantitation of [3-^{13}C]-pyruvate (*B*) and [2-^{13}C]-acetate (*C*). Data are shown as the mean ± SD of triplicates. (*D*) Lipid synthesis from glucose carbon in mock- and HCMV-infected HFs depleted of PDH E1α. HFs were treated with shGFP or shE1α as described, and lipid synthesis from [U-^{14}C]-D-glucose was measured in mock- and HCMV-infected cells as described in Fig. 1*D*. Data are shown as the mean ± SD of triplicates. (*E*) HCMV viral titers at 72 and 96 hpi in HFs treated with shGFP or shE1α as described in *A*.

histone acetylation, to regulate gene expression, and the sole donor of the acetyl groups for the neurotransmitter, acetylcholine (10). In mammalian cells, the cytosolic pool of Ac-CoA for lipid synthesis is made by ACLY and ACSS2 (13). In the presence of abundant nutrients, cells produce cytosolic Ac-CoA predominantly by converting mitochondria-derived citrate via the ACLY-mediated reaction (Fig. 1*A*); however, under nutrient-restricted conditions such as fasting or starvation, cytosolic Ac-CoA can be made from acetate by ACSS2 (33). It has been suggested that under normal conditions ACSS2 remains inactive, and the utilization of acetate carbon is low even if it is available (34). Under fasting conditions, caloric restriction signals the activation of the sirtuin (SIRT) family of NAD^+-dependent protein deacetylase to switch to fasting metabolism, resulting in decreased glucose utilization and increased utilization of other carbon sources, particularly acetate (35, 36). Some key changes in this switch are the deacetylation and activation of ACSS1 and ACSS2 by SIRT3 and SIRT1, respectively, resulting in the conversion of acetate to Ac-CoA by ACSS2 for lipid synthesis in the cytoplasm or by ACSS1 for entering the TCA cycle in the mitochondria (34, 37, 38).

Our studies show that loss of the utilization of citrate for Ac-CoA synthesis via the ACLY reaction has little effect on lipid synthesis and viral growth in HCMV-infected cells; the loss of ACLY can be completely compensated by acetate and the ACSS2 pathway, suggesting that HCMV infection may induce a fasting-like state of metabolic stress. As in HCMV-infected cells, lipogenesis is required in cancer cells to maintain proliferation. Interestingly, lipogenesis from glucose carbon in cancer cells is only slightly reduced by ACLY depletion (12). Further, recent studies have shown that in cancer cells the nutrient utilization is shifted significantly to acetate under metabolic-stress conditions, such as hypoxia, and the ACSS2 pathway is a major means of Ac-CoA synthesis to support lipogenesis under these conditions (15, 29). In this regard our previous studies have shown that HCMV infection is not altered significantly by metabolic stress such as hypoxia (39). Hence it appears that both HCMV infection and oncogenesis invoke the production of Ac-CoA from acetate via ACSS2 to promote lipogenesis.

A question that arises is the source of the acetate, especially in tissue culture, because acetate is not a component of tissue culture medium formulations. However, recent studies have shown that a low amount of acetate can be detected in fresh serum-free medium (29). Additionally, it has been proposed previously that pyruvate can be decomposed to acetate in sterile culture medium stored at 5 °C (40). In agreement, our studies show that in fresh, serum-free DMEM acetate can be derived from pyruvate. It is very unlikely that the ^{13}C-acetate detected comes from the contamination of metabolic tracers used in our labeling experiments: The supply of ^{13}C-acetate will be limited if it is a contamination, and therefore the level of ^{13}C-acetate from HCMV-infected HFs should not be higher than that from mock-infected HFs, as shown in Fig. 5 *B* and *E*; instead, much less ^{13}C-acetate should be detected in HCMV-infected HFs because of their much faster utilization of acetate. Thus, and because the same conversion does not occur in water, the conversion from ^{13}C-pyruvate to ^{13}C-acetate apparently is catalyzed by medium

components. For further confirmation of this idea, we tested the purity of [1,6-^{13}C2]-D-glucose and [3-^{13}C]-pyruvate. A stock solution of 5.6 mM [1,6-^{13}C2]-D-glucose dissolved in deuterated NMR solvent DMSO (DMSO-D6) was measured by NMR. No detectable ^{13}C-acetate was found in ^{13}C-glucose (Fig. S6*A*). Although a trace amount of [2-^{13}C]-acetate was detected in 1 mM [3-^{13}C]-pyruvate stock solution in DMSO-D6, it was 175-fold less than ^{13}C-pyruvate (Fig. S6*B*). This amount of [2-^{13}C]-acetate is approximately one-seventh to 1/13th of the [2-^{13}C]-acetate detected in medium (Fig. 5 *B* and *D*); therefore, it should not be considered the major source of the ^{13}C-acetate detected in medium.

Our data showed that the great majority of pyruvate in the cultured medium is generated intracellularly from glucose in both mock- and HCMV-infected HFs (Fig. S7*A*) and that infected HFs produced much higher levels of extracellular pyruvate than uninfected HFs (Fig. S7*B*). Because pyruvate can cross the cell membrane bidirectionally through facilitated transport by MCTs (41), it is reasonable that infected HFs would have higher levels of intracellular pyruvate than uninfected HFs. Our results showed that the intracellular level of pyruvate was increased in HFs infected with HCMV Towne strain (Fig. S7*C*). Further, in theory, every medium component should be present within cells. Therefore, the extracellular reaction that converts pyruvate to acetate very likely also happens intracellularly. Under in vitro culture conditions, and presumably in vivo, this reaction would allow glucose carbon to be converted to acetate via the glycolytic production of pyruvate. Thereafter the glucose-derived acetate would be converted to Ac-CoA by ACSS2.

In addition, there are many other sources of acetate within cells (e.g., the deacetylation of histones and other acetylated proteins) and within the body (e.g., circulating acetate from sources such as the gut microbiota). In the experiment of ^{13}C-glucose labeling shown in Fig. 5*E*, we found that acetate produced from glucose carbon was only 40% of total acetate released from uninfected HFs, but in HCMV-infected cells, this level was increased to 60% (Fig. S7*D*), although almost 90% of pyruvate was made from glucose in both mock- and HCMV-infected HFs (Fig. S7*A*). These data suggest that multiple mechanisms function to generate acetate and that HCMV infection can enhance acetate production from glucose. These multiple sources may provide an abundant supply of acetate, making the acetate/ACSS2 pathway the preferred means of Ac-CoA production to support lipogenesis in cancer cells and HCMV-infected cells.

Studies from several laboratories have indicated that pyruvate has antioxidant capacity to prevent oxidant-induced apoptosis in mammalian cells (42–45). A more recent NMR study has shown that reaction of sodium pyruvate with hydrogen peroxide generates acetate, CO_2 and H_2O (46). Reactive oxygen species (ROS) are natural byproducts generated from normal metabolic activities (47). Cellular ROS needs to be tightly controlled; otherwise high ROS levels may result in significant damage to cell structures, including DNA damage, lipid peroxidation, oxidations of amino acids in proteins, deactivation of specific enzymes by oxidation of cofactors, and others, to induce apoptosis (48). Previously, our laboratory has shown that HCMV can activate multiple means of protecting cells from ROS stress to favor its efficient replication (49). It is possible that increased glycolysis and pyruvate production is another mean used by HCMV for protection from ROS stress and to ensure the success of infection.

Materials and Methods

Cells, Viruses, and Reagents. Primary and life-extended human foreskin fibroblasts (HFs) (50) were propagated and maintained in DMEM supplemented with 10% (vol/vol) FCS, 100 U/mL penicillin, 100 μg/mL streptomycin, and 2 mM GlutaMAX (all reagents were obtained from Invitrogen). For isotope labeling and nutrient experiments, the base DMEM lacking glucose, glutamine, and pyruvate (D5030; Sigma) was used. The D5030 medium was supplemented with antibiotics, 4 mM glutamine, and 5.6 mM glucose or 1 mM pyruvate, as needed. For metabolic labeling experiments, [1, 6-^{13}C2]-D-glucose (CLM-2717; Cambridge Isotope Laboratories) and [3-^{13}C]-pyruvate (CLM-1575; Cambridge Isotope Laboratories) were used to replace glucose in D5030 medium. For the lipid synthesis assay, [U-^{14}C]-D-glucose and [1, 2-^{14}C2]-acetate were purchased from Moravek Biochemicals.

The following antibodies were used to detect proteins by Western bolt analysis: anti-actin (MAB1501; Chemicon), anti-ACLY (15421-1-AP; Proteintech Group), anti-ACSS2 (3658; Cell Signaling Technology), anti-PDH E1α (ab110330; Abcam), anti-pp28 (sc-56975; Santa Cruz), anti-pp52 (sc-69744; Santa Cruz), anti-pp65 (sc-52401; Santa Cruz), and anti-ex2/3 (antibody against IE72 and IE86) (51).

HCMV (Towne strain) stocks with or without the cassette expressing GFP were prepared and purified as previously described (39). All HCMV experiments were performed in serum-starved HFs by infection with HCMV Towne at an MOI of 3. The viral growth assay was performed as previously described (26).

Cloning of ACLY- and ACSS2-KO HF Cells Using CRISPR/Cas9 Technology. sgRNA sequences specific for the human genes *ACLY* and *ACSS2* were cloned into LentiCRISPR-v2 (52, 53), a lentiviral vector coexpressing a mammalian codon-optimized Cas9 nuclease along with an sgRNA. An sgRNA sequence specific for the firefly luciferase gene was also used to make control HFs. Sequence information for sgRNAs is listed in Table S1. Lentiviruses expressing Cas9 and sgRNAs were produced in 293T cells and were used to transduce HFs. Transduced HFs were diluted and seeded at one or two cells per well in 96-well plates which were overlaid with ∼200 nontransduced HFs per well. HFs were cultured in normal medium for ∼7–10 d until 90% confluence, followed by culturing in selection medium containing 1.0 μg/mL puromycin. Puromycin-resistant HF clones were analyzed by Western blot. Gene modification by CRISPR was verified by PCR and the sequencing of targeting genomic regions using primers listed in Table S2. Genetically validated HF clones were used for further lipid synthesis and viral growth assays.

shRNA Depletion Experiments. Lentiviral vectors expressing shGFP, shACLY (TRCN0000078285), shE1α-A (TRCN0000028582 + TRCN0000028627), and shE1α-B (TRCN0000028627 + TRCN0000028630) were made as described previously (54). Subconfluent HFs were infected with lentiviral vectors in the presence of 8 μg/mL polybrene (Sigma) for 2 h, followed by replacement with fresh complete DMEM medium. After culture for another 3 d in fresh medium, cells were serum-starved for 1 d and then were infected with HCMV (at an MOI of 3) in serum-free DMEM for the designed assays.

Lipid Synthesis Assay. Total lipid synthesis from glucose or acetate carbon was measured by labeling HFs with [1, 2-^{14}C2]-acetate or [U-^{14}C]-D-glucose. Briefly, at 48 hpi mock- and HCMV-infected HFs were labeled with 1.0 μCi/mL [U-^{14}C]-D-glucose for 24 h in serum-free D5030 medium supplemented with 5.6 mM glucose and 4 mM glutamine. For acetate utilization in lipid synthesis, the mock-infected or infected HFs were labeled with 1.0 μCi/mL [1, 2-^{14}C2]-acetate in DMEM for 2 h. After either glucose or acetate labeling, total lipids were extracted and counted in a scintillation counter (Beckman Coulter) as described previously (6). *P* values were determined by the Student's paired *t* test with two-tailed distribution.

Lipid Droplet Staining. Cellular lipid droplets were stained with BODIPY 558/568 C_{12} [4,4-difloro-5-(2-thienyl)-4-bora-3a,4a-diaza-*s*-indacene-3-dodecanoic acid] (Molecular Probes) as previously described (6). Briefly, the cells in 35-mm dishes were incubated with 10 μg/mL BODIPY 558/568 C_{12} for 45 min at 37 °C in serum-free DMEM. The cells were washed once with serum-free DMEM and refed with fresh DMEM for a further incubation of 45–60 min at 37 °C. Then the cells were fixed with 4% (wt/vol) paraformaldehyde for 30 min at room temperature, washed with PBS, and mounted using VECTASHIELD containing DAPI. The images were captured at the same microscopy exposure setting.

NMR Spectroscopy. All NMR spectra were acquired using a Bruker Avance III HD NMR spectrometer equipped with a triple-resonance inverse (TXI) 3-mm probe (Bruker BioSpin). To ensure high throughput, a Bruker SampleJet was used for sample handling. For all 1D NMR spectra, the pulse program took the shape of the first transient of a 2D NOESY and generally of the form RD-90-t-90-t_m-90-ACQ (55), where *RD* = relaxation delay, *t* = small time delay between pulses, t_m = mixing time, and *ACQ* = acquisition. The water signal was saturated using continuous irradiation during the relaxation delay and mixing time. The spectra were acquired using 76,000 data points and a spectral width of 14 ppm. Sixty-four scans were performed with a 1-s interscan (relaxation) delay, and 0.1-s mixing time was allowed. The free induction decays (FIDs) were zero filled to 128,000; 0.1 Hz of linear broadening

was applied followed by Fourier transformation and baseline and phase correction using an automated program provided by Bruker BioSpin.

To prepare samples for NMR, 180 μL of sample was added to 20 μL of 4,4-Dimethyl-4-silapentane-1-sulfonic acid (DSS) (Cambridge Isotope Laboratories) so that the final concentration of DSS was ~0.25 mM. These samples were transferred into 3-mm SampleJet rack NMR tubes (Bruker BioSpin). The acetate signal was profiled from the spectra using Chenomx v. 8.0 (56). For experiments involving no ^{13}C-labeled precursor, the acetate signal at 1.90 ppm was quantified. To quantify the ^{13}C-acetate from experiments involving ^{13}C-precursors, satellite peaks were identified in the spectra and were quantified.

ACKNOWLEDGMENTS. We thank all members of the J.C.A. laboratory and Kathryn Wellen for technique support and helpful discussions. This research was supported by NIH Grants R21 AI105679 (to Y.Y.) and R01 CA157679 (to J.C.A.).

1. Pass RF, Fowler KB, Boppana SB, Britt WJ, Stagno S (2006) Congenital cytomegalovirus infection following first trimester maternal infection: Symptoms at birth and outcome. *J Clin Virol* 35(2):216–220.
2. Rowshani AT, Bemelman FJ, van Leeuwen EM, van Lier RA, ten Berge IJ (2005) Clinical and immunologic aspects of cytomegalovirus infection in solid organ transplant recipients. *Transplantation* 79(4):381–386.
3. Hibberd PL, Snydman DR (1995) Cytomegalovirus infection in organ transplant recipients. *Infect Dis Clin North Am* 9(4):863–877.
4. Popović M, et al. (2012) Human cytomegalovirus infection and atherothrombosis. *J Thromb Thrombolysis* 33(2):160–172.
5. Michaelis M, Doerr HW, Cinatl J (2009) The story of human cytomegalovirus and cancer: Increasing evidence and open questions. *Neoplasia* 11(1):1–9.
6. Yu Y, Maguire TG, Alwine JC (2012) Human cytomegalovirus infection induces adipocyte-like lipogenesis through activation of sterol regulatory element binding protein 1. *J Virol* 86(6):2942–2949.
7. Munger J, et al. (2008) Systems-level metabolic flux profiling identifies fatty acid synthesis as a target for antiviral therapy. *Nat Biotechnol* 26(10):1179–1186.
8. Spencer CM, Schafer XL, Moorman NJ, Munger J (2011) Human cytomegalovirus induces the activity and expression of acetyl-coenzyme A carboxylase, a fatty acid biosynthetic enzyme whose inhibition attenuates viral replication. *J Virol* 85(12):5814–5824.
9. Yu Y, Maguire TG, Alwine JC (2014) ChREBP, a glucose-responsive transcriptional factor, enhances glucose metabolism to support biosynthesis in human cytomegalovirus-infected cells. *Proc Natl Acad Sci USA* 111(5):1951–1956.
10. Pietrocola F, Galluzzi L, Bravo-San Pedro JM, Madeo F, Kroemer G (2015) Acetyl coenzyme A: A central metabolite and second messenger. *Cell Metab* 21(6):805–821.
11. Bauer DE, Hatzivassiliou G, Zhao F, Andreadis C, Thompson CB (2005) ATP citrate lyase is an important component of cell growth and transformation. *Oncogene* 24(41):6314–6322.
12. Hatzivassiliou G, et al. (2005) ATP citrate lyase inhibition can suppress tumor cell growth. *Cancer Cell* 8(4):311–321.
13. Wellen KE, et al. (2009) ATP-citrate lyase links cellular metabolism to histone acetylation. *Science* 324(5930):1076–1080.
14. Mashimo T, et al. (2014) Acetate is a bioenergetic substrate for human glioblastoma and brain metastases. *Cell* 159(7):1603–1614.
15. Schug ZT, et al. (2015) Acetyl-CoA synthetase 2 promotes acetate utilization and maintains cancer cell growth under metabolic stress. *Cancer Cell* 27(1):57–71.
16. Comerford SA, et al. (2014) Acetate dependence of tumors. *Cell* 159(7):1591–1602.
17. Buckley BM, Williamson DH (1977) Origins of blood acetate in the rat. *Biochem J* 166(3):539–545.
18. Scheppach W, Pomare EW, Elia M, Cummings JH (1991) The contribution of the large intestine to blood acetate in man. *Clin Sci (Lond)* 80(2):177–182.
19. Lundquist F, Tygstrup N, Winkler K, Mellemgaard K, Munck-Petersen S (1962) Ethanol metabolism and production of free acetate in the human liver. *J Clin Invest* 41:955–961.
20. Sadoul K, Boyault C, Pabion M, Khochbin S (2008) Regulation of protein turnover by acetyltransferases and deacetylases. *Biochimie* 90(2):306–312.
21. Tomaszewicz M, Rossner S, Schliebs R, Cwikowska J, Szutowicz A (2003) Changes in cortical acetyl-CoA metabolism after selective basal forebrain cholinergic degeneration by 192IgG-saporin. *J Neurochem* 87(2):318–324.
22. Bernson SM, Nicholls DG (1974) Acetate, a major end product of fatty-acid oxidation in hamster brown-adipose-tissue mitochondria. *Eur J Biochem* 47(3):517–525.
23. Yu Y, Maguire TG, Alwine JC (2011) Human cytomegalovirus activates glucose transporter 4 expression to increase glucose uptake during infection. *J Virol* 85(4):1573–1580.
24. Berwick DC, Hers I, Heesom KJ, Moule SK, Tavare JM (2002) The identification of ATP-citrate lyase as a protein kinase B (Akt) substrate in primary adipocytes. *J Biol Chem* 277(37):33895–33900.
25. Pierce MW, Palmer JL, Keutmann HT, Hall TA, Avruch J (1982) The insulin-directed phosphorylation site on ATP-citrate lyase is identical with the site phosphorylated by the cAMP-dependent protein kinase in vitro. *J Biol Chem* 257(18):10681–10686.
26. Yu Y, Pierciey FJ, Jr, Maguire TG, Alwine JC (2013) PKR-like endoplasmic reticulum kinase is necessary for lipogenic activation during HCMV infection. *PLoS Pathog* 9(4):e1003266.
27. Takahashi H, McCaffery JM, Irizarry RA, Boeke JD (2006) Nucleocytosolic acetyl-coenzyme a synthetase is required for histone acetylation and global transcription. *Mol Cell* 23(2):207–217.
28. Alves MG, et al. (2012) In vitro cultured human Sertoli cells secrete high amounts of acetate that is stimulated by 17β-estradiol and suppressed by insulin deprivation. *Biochim Biophys Acta* 1823(8):1389–1394.
29. Yoshii Y, et al. (2009) Cytosolic acetyl-CoA synthetase affected tumor cell survival under hypoxia: The possible function in tumor acetyl-CoA/acetate metabolism. *Cancer Sci* 100(5):821–827.
30. Kamphorst JJ, Chung MK, Fan J, Rabinowitz JD (2014) Quantitative analysis of acetyl-CoA production in hypoxic cancer cells reveals substantial contribution from acetate. *Cancer Metab* 2:23.
31. Mancuso A, Sharfstein ST, Tucker SN, Clark DS, Blanch HW (1994) Examination of primary metabolic pathways in a murine hybridoma with carbon-13 nuclear magnetic resonance spectroscopy. *Biotechnol Bioeng* 44(5):563–585.
32. Rajagopalan KN, et al. (2015) Metabolic plasticity maintains proliferation in pyruvate dehydrogenase deficient cells. *Cancer Metab* 3:7.
33. Li Y, et al. (2016) PDHA1 gene knockout in prostate cancer cells results in metabolic reprogramming towards greater glutamine dependence. *Oncotarget* 7(33):53837–53852.
34. Wellen KE, Thompson CB (2012) A two-way street: Reciprocal regulation of metabolism and signalling. *Nat Rev Mol Cell Biol* 13(4):270–276.
35. Hallows WC, Lee S, Denu JM (2006) Sirtuins deacetylate and activate mammalian acetyl-CoA synthetases. *Proc Natl Acad Sci USA* 103(27):10230–10235.
36. Houtkooper RH, Pirinen E, Auwerx J (2012) Sirtuins as regulators of metabolism and healthspan. *Nat Rev Mol Cell Biol* 13(4):225–238.
37. Newman JC, He W, Verdin E (2012) Mitochondrial protein acylation and intermediary metabolism: Regulation by sirtuins and implications for metabolic disease. *J Biol Chem* 287(51):42436–42443.
38. Hirschey MD, Shimazu T, Capra JA, Pollard KS, Verdin E (2011) SIRT1 and SIRT3 deacetylate homologous substrates: AceCS1,2 and HMGCS1,2. *Aging (Albany NY)* 3(6):635–642.
39. Schwer B, Bunkenborg J, Verdin RO, Andersen JS, Verdin E (2006) Reversible lysine acetylation controls the activity of the mitochondrial enzyme acetyl-CoA synthetase 2. *Proc Natl Acad Sci USA* 103(27):10224–10229.
40. Kudchodkar SB, Yu Y, Maguire TG, Alwine JC (2004) Human cytomegalovirus infection induces rapamycin-insensitive phosphorylation of downstream effectors of mTOR kinase. *J Virol* 78(20):11030–11039.
41. Wales RG, Whittingham DG (1971) Decomposition of sodium pyruvate in culture media stored at 5 degrees C and its effects on the development of the preimplantation mouse embryo. *J Reprod Fertil* 24(1):126.
42. Lee YJ, Kang IJ, Bünger R, Kang YH (2003) Mechanisms of pyruvate inhibition of oxidant-induced apoptosis in human endothelial cells. *Microvasc Res* 66(2):91–101.
43. Kang YH, Chung SJ, Kang IJ, Park JH, Bünger R (2001) Intramitochondrial pyruvate attenuates hydrogen peroxide-induced apoptosis in bovine pulmonary artery endothelium. *Mol Cell Biochem* 216(1-2):37–46.
44. Ramakrishnan N, Chen R, McClain DE, Bünger R (1998) Pyruvate prevents hydrogen peroxide-induced apoptosis. *Free Radic Res* 29(4):283–295.
45. Herz H, Blake DR, Grootveld M (1997) Multicomponent investigations of the hydrogen peroxide- and hydroxyl radical-scavenging antioxidant capacities of biofluids: The roles of endogenous pyruvate and lactate. Relevance to inflammatory joint diseases. *Free Radic Res* 26(1):19–35.
46. Asmus C, Mozziconacci O, Schöneich C (2015) Low-temperature NMR characterization of reaction of sodium pyruvate with hydrogen peroxide. *J Phys Chem A* 119(6):966–977.
47. Turrens JF (2003) Mitochondrial formation of reactive oxygen species. *J Physiol* 552(Pt 2):335–344.
48. Finkel T (2003) Oxidant signals and oxidative stress. *Curr Opin Cell Biol* 15(2):247–254.
49. Tilton C, Clippinger AJ, Maguire T, Alwine JC (2011) Human cytomegalovirus induces multiple means to combat reactive oxygen species. *J Virol* 85(23):12585–12593.
50. Bresnahan WA, Hultman GE, Shenk T (2000) Replication of wild-type and mutant human cytomegalovirus in life-extended human diploid fibroblasts. *J Virol* 74(22):10816–10818.
51. Harel NY, Alwine JC (1998) Phosphorylation of the human cytomegalovirus 86-kilodalton immediate-early protein IE2. *J Virol* 72(7):5481–5492.
52. Sanjana NE, Shalem O, Zhang F (2014) Improved vectors and genome-wide libraries for CRISPR screening. *Nat Methods* 11(8):783–784.
53. Shalem O, et al. (2014) Genome-scale CRISPR-Cas9 knockout screening in human cells. *Science* 343(6166):84–87.
54. Yu Y, Alwine JC (2008) Interaction between simian virus 40 large T antigen and insulin receptor substrate 1 is disrupted by the K1 mutation, resulting in the loss of large T antigen-mediated phosphorylation of Akt. *J Virol* 82(9):4521–4526.
55. Beckonert O, et al. (2007) Metabolic profiling, metabolomic and metabonomic procedures for NMR spectroscopy of urine, plasma, serum and tissue extracts. *Nat Protoc* 2(11):2692–2703.
56. Weljie AM, Newton J, Mercier P, Carlson E, Slupsky CM (2006) Targeted profiling: Quantitative analysis of 1H NMR metabolomics data. *Anal Chem* 78(13):4430–4442.
57. Luong A, Hannah VC, Brown MS, Goldstein JL (2000) Molecular characterization of human acetyl-CoA synthetase, an enzyme regulated by sterol regulatory element-binding proteins. *J Biol Chem* 275(34):26458–26466.
58. Sancak Y, et al. (2008) The Rag GTPases bind raptor and mediate amino acid signaling to mTORC1. *Science* 320(5882):1496–1501.